

# Optical and control modeling for adaptive beam-combining experiments

J.K. Gruetzner

S.D. Tucker

D.R. Neal

A.E. Bentley

K. Simmons-Potter

*Sandia National Laboratories, Org. 1128, MS 1423*

*PO Box 5800, Albuquerque, NM 87185-1423*

*e-mail: jkgruet@sandia.gov*

*(505) 844-9508*

## ABSTRACT

The development of modeling algorithms for adaptive optics systems is important for evaluating both performance and design parameters prior to system construction. Two of the most critical sub-systems to be modeled are the binary optic design and the adaptive control system. Since these two are intimately related, it is beneficial to model them simultaneously.

Optic modeling techniques have some significant limitations. Diffraction effects directly limit the utility of geometrical ray-tracing models, and transform techniques such as the fast fourier transform can be both cumbersome and memory intensive. We have developed a hybrid system incorporating elements of both ray-tracing and fourier transform techniques.

In this paper we present an analytical model of wavefront propagation through a binary optic lens system developed and implemented at Sandia. This model is unique in that it solves the transfer function for each portion of a diffractive optic analytically. The overall performance is obtained by a linear superposition of each result. The model has been successfully used in the design of a wide range of binary optics, including an adaptive optic for a beam combining system consisting of an array of rectangular mirrors, each controllable in tip/tilt and piston.

Wavefront sensing and the control models for a beam combining system have been integrated and used to predict overall systems performance. Applicability of the model for design purposes is demonstrated with several lens designs through a comparison of model predictions with actual adaptive optics results.

**Keywords:** adaptive optic, binary optic, optic modelling, adaptive optic control systems, coherent beam combining

# 1 INTRODUCTION

In the field of adaptive optics, modeling algorithms for the optical and control systems are important for evaluating both performance and design parameters prior to system construction. The correspondence of the predicted with the actual results is a measure of the usefulness of the model in explaining or predicting what occurs. To be useful, the model must predict the actual performance to within an adequate degree of accuracy. For control systems, the speed at which the model operates can also be a factor. It may be beneficial to develop more than one model of the same component, each model serving a specific purpose.

Binary optics are optical components (e.g., lenses) fabricated using semiconductor manufacturing methods. For an adaptive optics system using binary optics, two important subsystems to be modeled are the binary optic design and the control system. It is advantageous to have two models of the optic performance: a thorough and accurate model for the optic design, and a faster model with adequate precision for use in developing the control system.

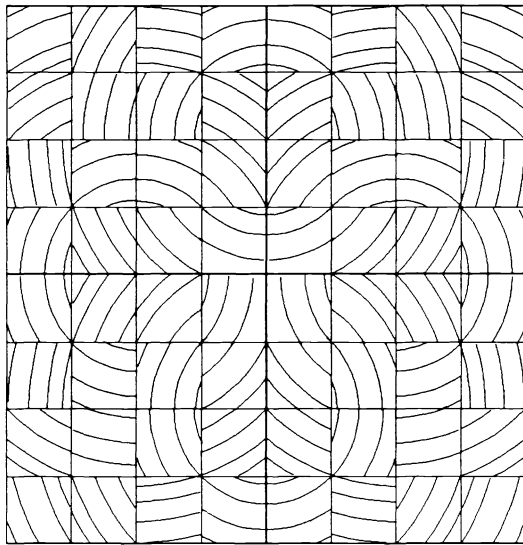
# 2 OPTICS MODELING

Diffraction binary optics fabricated at Sandia use processes similar to those used in integrated circuit manufacture. The optic is laid out using a computer-assisted drafting (CAD) program and transferred to a series of photo-masks, each mask representing a detail of the lens structure. The optic profile is built up by reactive-ion etching of the pattern into a dielectric substrate, with the process repeated  $N$  times with different masks and halving the etch depth with each step. We have typically used  $N = 4$  masks, resulting in optic structures with 16 levels. This is further described in other work.<sup>1,2</sup> Binary optics fabrication techniques such as this can produce optics with  $\sim 1\mu m$  feature size, these features being completely arbitrary.<sup>3,4</sup>

The binary optics for certain adaptive optical systems developed at Sandia use aperture multiplexing.<sup>4</sup> In this approach, the optical aperture is broken up into a series of small segments, or *facets*. (See Figure 1.) Each facet can be designed to be a portion of a specific lens—termed a *lenslet*—with a peculiar focal point relative to the entire aperture. In addition, each facet samples the incoming wavefront for a portion of the total aperture. If these samples are small enough, they may be focused to different spots on a detector at the focal plane, mimicking the performance of a lens covering the entire aperture from which samples are drawn. The overall pattern on the detector is the coherent sum of the field produced by all the individual facets.

Figure 1 depicts an optic of this type which might be used as a matrix phase comparator.<sup>2</sup> In this instrument, the relative phases of four laser beams are compared. Each beam passes through one quadrant of the optic. Adjacent beams are imaged to a spot on the detector (image plane) on the quadrant boundary. This produces an interference pattern, based upon the phase difference between the adjacent beams. The result is similar to that which would result from the superposition of two lenses per quadrant, each focusing to a different boundary.

In beam-combining, the interference patterns produced are analyzed to determine this phase difference; the result is an input into an adaptive optic system which, using a set of mirrors, adjusts the piston—and thereby the phase—of the beams as required towards a goal of zero phase difference between beams. If the four beams are coplanar, as brought about by a different sensor, the resultant combination of the four beams is a coherent beam of four times the area of a single beam. Since the intensity of the overall beam is the square of the coherent sum of the fields of the individual beams,



Binary optic showing facets

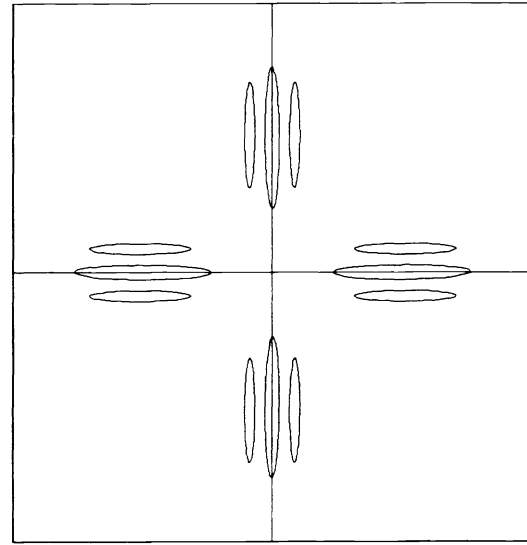


Image plane showing interference fringes

Figure 1: Arrangement for four-beam phase comparator. Each beam passes through a given quadrant. There are 16  $4 \times 4$  facets per quadrant, with the facets forming part of four different lenses. Adjacent beams are interfered at lens focal points.

this maximizes the combined beam intensity and thereby the power transmitted by the beams.

Paraxial or geometric ray tracing is not a suitable modeling technique for this type of optic. This is primarily due to the effects of diffraction and interference, which directly limit the utility of these models. Because aperture multiplexing creates aperture patterns (the facets) that are small, careful diffraction analysis is important. Not only does the diffraction from the entire aperture have to be considered, but also the diffraction from each individual facet must be accounted for. This is especially true of systems which exploit the interference of two separate beams to obtain a measurement.

Discrete transform techniques, such as the fast Fourier transform (FFT), proved awkward in our initial modeling attempts, mainly due to the multi-faceted nature of each lenslet. In order to obtain sufficient guardbands for a two-dimensional transform, computer memory requirements soon outstripped the memory available on a standard personal computer. The increased number of calculations required also led to an increase in processing time. This served as an impetus to develop a model which would be more conservative of computer resources and faster in computation time.

## 2.1 Analytical model

The vast majority of binary optics produced by our group at Sandia can be analyzed in terms of rectangular facets. The light from each facet produces an electric field intensity at a focal plane common to all facets. The focal plane electric field produced by light from the entire binary optic is the superposition of the field of each facet. The intensity pattern is, of course, proportional to the square of the magnitude of the total electric field.<sup>4</sup>

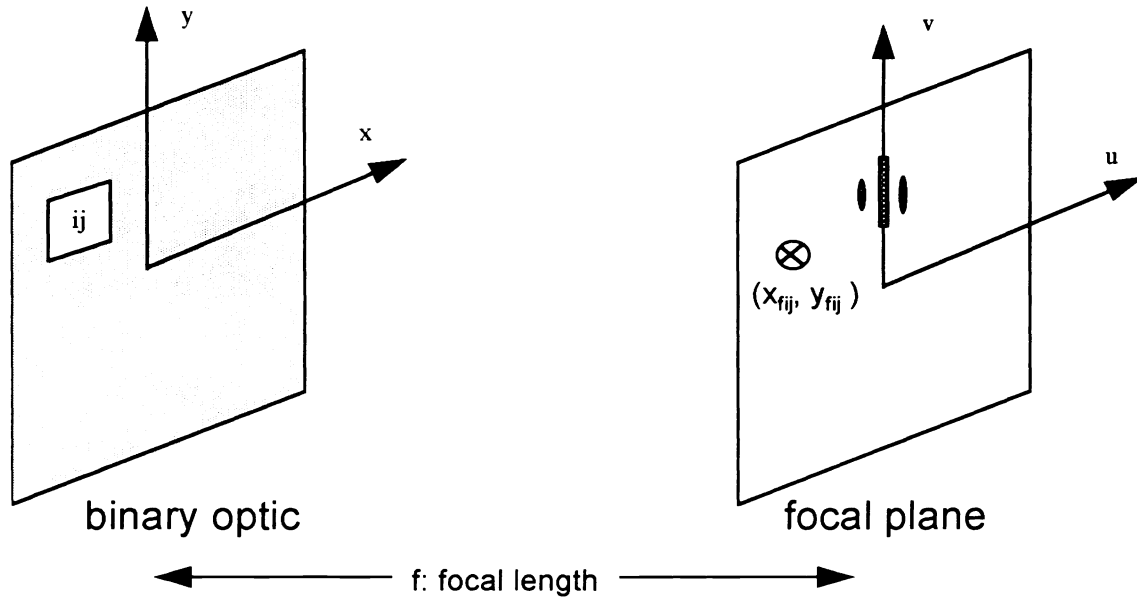


Figure 2: Model calculation geometry. Diffraction from each facet  $ij$  is summed to provide the intensity pattern as  $x_{f_{ij}}, y_{f_{ij}}$ .

The geometry of Figure 2 is used in our analysis. For each facet (indicated by indices  $i$  and  $j$ ), phase information for the zeroth (piston) and first (tip/tilt) order of the wavefront are used as input to the model. This corresponds to the complex-valued transmission function of the facet. Using the Fourier transforming and imaging properties of lenses, standard analysis techniques<sup>5</sup> modified for the geometry shown are used to obtain an integral expression for the electric field due to light from an individual facet. Due to the specific nature of the geometry, this integral can be solved analytically in terms of trigonometric functions. The complex-valued electric field produced by the  $ij$ -th facet at a point  $u, v$  on the image plane is

$$\begin{aligned} \tilde{E}_{ij}(u, v) = & \sqrt{I_{ij}} \frac{ab}{i\lambda f} \exp \left[ \frac{2\pi i}{\lambda} (f + \epsilon_{ij}) \right] \times \\ & \text{sinc} \left( \frac{\pi a}{\lambda f} (u - f \theta_{ij} - x_{f_{ij}}) \right) \times \\ & \text{sinc} \left( \frac{\pi b}{\lambda f} (v - f \psi_{ij} - y_{f_{ij}}) \right) \times \\ & \exp \left[ \frac{\pi i}{\lambda f} \left( u^2 - x_{f_{ij}}^2 - 2x_{ij} (u - x_{f_{ij}}) \right) \right] \times \\ & \exp \left[ \frac{\pi i}{\lambda f} \left( v^2 - y_{f_{ij}}^2 - 2y_{ij} (v - y_{f_{ij}}) \right) \right], \end{aligned} \quad 1$$

where  $\sqrt{I_{ij}}$  is the average input wave amplitude,  $f$  the lenslet focal length,  $a$  and  $b$  are the horizontal and vertical facet dimensions,  $x_{ij}, y_{ij}$  are the coordinates of the facet center,  $x_{f_{ij}}, y_{f_{ij}}$  are the coordinates of the focus point,  $\epsilon_{ij}$  is the average wavefront advancement (piston), and  $\theta_{ij}, \psi_{ij}$  are the average  $x$ - and  $y$ -tilt respectively. Note that this replaces the model of previous work<sup>4</sup> where the aberrations could not be handled correctly. The intensity pattern at the focal plane produced by a binary optic of  $N$  by  $M$  facets is then

$$I(u, v) = \left| \sum_{i=1}^N \sum_{j=1}^M \tilde{E}_{ij}(u, v) \right|^2. \quad 2$$

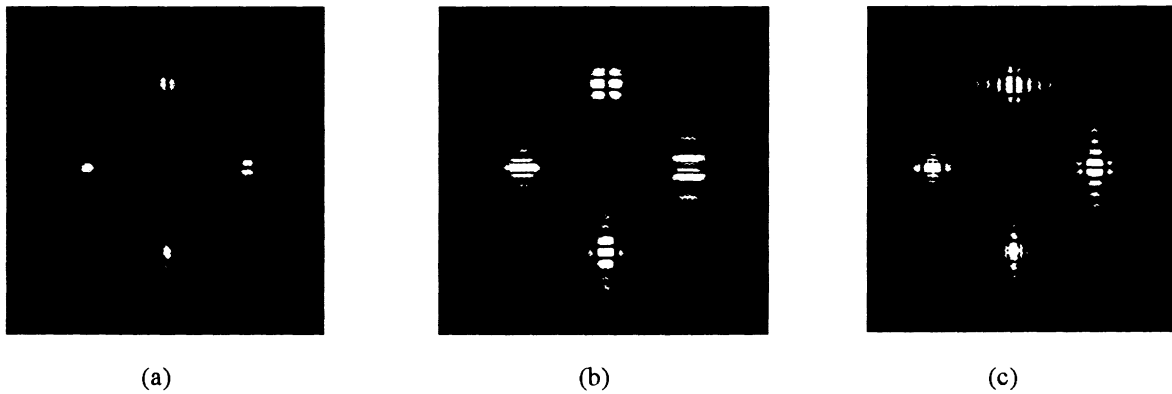


Figure 3: Image plane from model of three different binary optics. Each optic and its image is  $1 \text{ mm} \times 1 \text{ mm}$ . In each case, a plane wave is incident on the optic, with the upper right quadrant of each having a piston of one-half wave. (a) Image from the optic represented in Figure 1. (b) Image from a  $16 \times 16$  facet binary optic with a regular facet arrangement. (c) Image from a  $32 \times 32$  facet binary optic with a more irregular distribution of facets.

Due to the matrix nature of the problem, a vectorized, matrix-oriented language, MATLAB,<sup>6</sup> was chosen. This type of language has an advantage over programming languages, such as C, in reduced programming time and improved readability. With care taken to use vectorization programming techniques, speed of execution remains reasonable and approaches that of straight C code. However, we still did not find the speed of this model adequate to be useful for control system modeling.

The analytical model was found to run significantly faster than a commercial diffraction modeling program which used fast Fourier transforms (FFTs). When run on an IBM-clone personal computer (Intel 486 processor at 66 MHz clock speed), the FFT analysis took approximately  $2\frac{1}{2}$  hours per run for a 64-facet, 5-focus point design. The analytical model described above, when run on a slower PC (Intel 386 processor, 33 MHz clock speed) takes just over seven minutes. When ported to a Pentium PC, the analytical model requires less than a minute, including set-up time. Since the analytical model showed such an increase in speed that further use of the FFT model was halted.

The analytic model is of greatest use during the design phase of an aperture-multiplexing binary optic. The concept was initially applied to a wavefront sensor design,<sup>4</sup> where its validity was strongly supported. We have since applied it to other types of sensors with correspondingly good results.

Figure 3 shows model results of the intensity pattern at the focal plane for three possible phase comparator designs. Each image corresponds to the light intensity at the focal plane for a given design. The leftmost image is an  $8 \times 8$  facet design, with the facets arranged as shown in Figure 1. The image is the interference pattern produced by a plane wave with the upper-right quadrant having a piston offset of one-half wave. Note that the interference pattern between the shifted quadrant and the adjacent quadrants shows a null along the boundary axis, whereas quadrants which are in phase produce maxima along their respective boundaries.

The center image is of a  $16 \times 16$  facet optic, with the facets arranged in a regular order. The regular pattern produces unwanted interference fringes and a "smearing" of the pattern. The rightmost image is of a  $32 \times 32$  facet optic with a less regular facet pattern. Note that the interference pattern is usable out to a larger number of maxima and that the smearing effect is reduced.

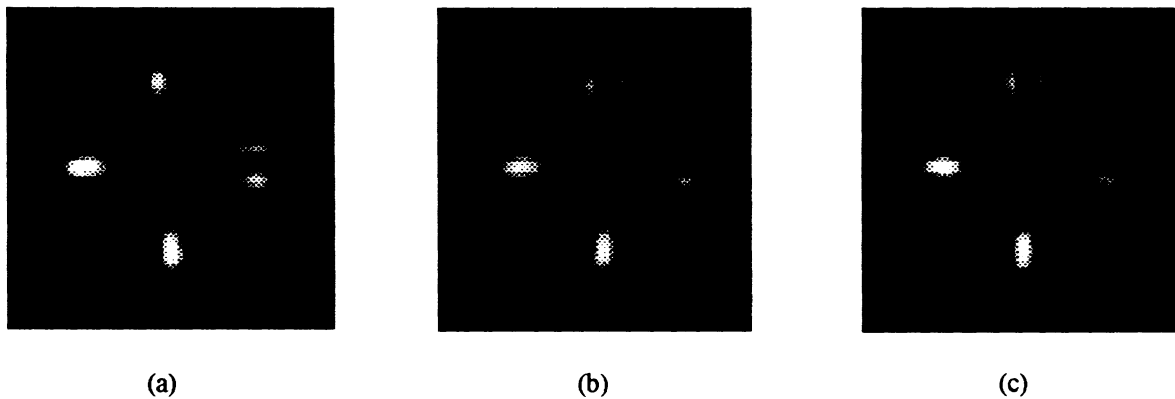


Figure 4: **Analytical model images for three possible phase comparator designs. Each image represents a  $1\text{mm} \times 1\text{mm}$  CCD camera array. The model was used to determine the minimum number of facets required to produce an adequate image. The optics modeled are  $16 \times 16$  facets,  $32 \times 32$  facets, and  $64 \times 64$  facets, for (a) through (c), respectively.**

Use of the model in minimizing the number of facets per beam to obtain an adequate image is demonstrated in Figure 4. The leftmost image, (a), is a  $16 \times 16$  facet design. Although it produces a recognizable fringe pattern, it is readily apparent that the  $32 \times 32$  facet design, (b) is an improvement. It is also apparent that the  $64 \times 64$  facet design of (c) offers little improvement for the increase in design and manufacturing complexity.

The beam-combining program at Sandia has explored the use of several different types of phase comparator systems, which determine phase differences between adjacent optical beams which are to be combined. These are explained in more detail in other work.<sup>2</sup> Two types are of particular interest. A *hierarchical* phase comparator consists of  $n$  tiers of comparison. It is used to combine  $2^{2n}$  beams, arranged in a square, into one coherent beam, with phase comparisons made by quadrant (first tier), then within each quadrant again by quadrant (second tier), etc. This lets the control system treat each quadrant (or subquadrant) as a single beam. A *matrix* phase comparator, on the other hand, compares only the phases of adjacent beam: it is these phase differences which then are inputs to the control algorithm.

This model has been successfully used in the design of both types Figure 5 shows far field images from a hierarchical phase comparator design. The image on the left was obtained in the laboratory from a comparator constructed using binary optic techniques. This closely matches the image on the right, which is the output from an analytical model used in the design of that binary optic. In both cases the impinging wave was basically planar. The slight difference between the two images was later traced to extraneous light noise in the CCD camera. Only a portion of the total image field was necessary to be modeled in order to validate the faceting scheme to be used.

A fortuitous instance showing the importance of modeling a design occurred in the manufacture of a recent binary optic. Due to the small size of these optics (usually 4mm on a side or less), it is customary to manufacture many different optics on the same substrate. Prior to production it was noticed that an additional  $4\text{mm} \times 4\text{mm}$  binary optic could be fit one of the substrates. An experienced binary optic designer was tasked with designing a  $128 \times 128$  facet,  $8 \times 8$  beam matrix phase comparator. Due to various constraints, an analytical model of the optic was not done until after the etch masks were created. The results are shown in Figure 6. The CCD camera image and the analytical model image are quite similar, and include a significant amount of spurious diffraction. The optic was still usable in

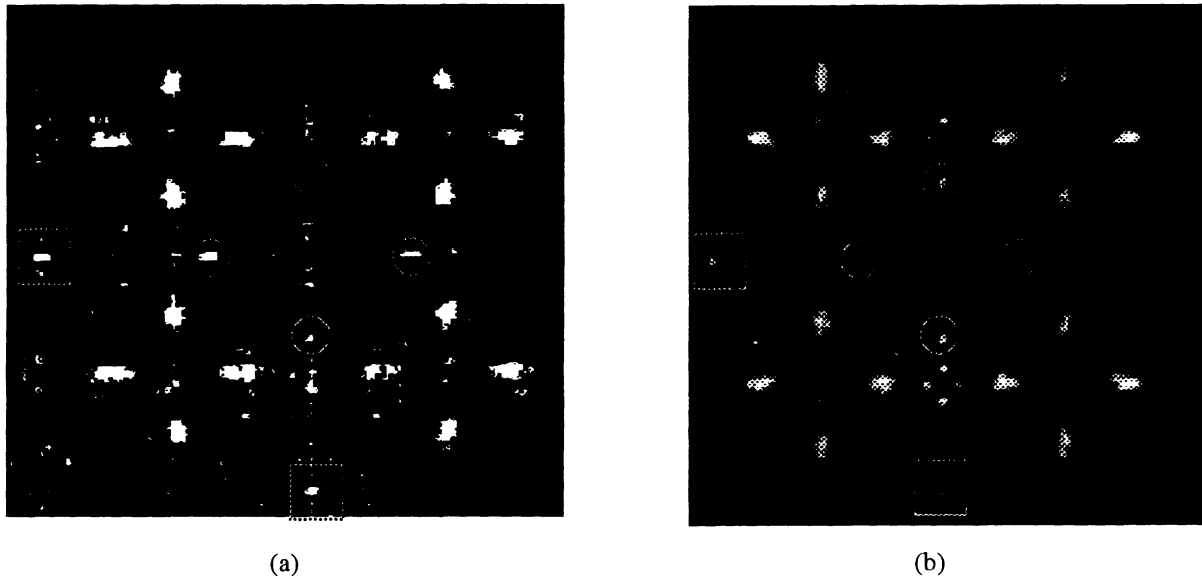


Figure 5: Use of model in design of a hierarchical phase comparator. Image (a) is the upper-right quadrant of the image plane of a three-tiered binary optic. (Since an autogain camera was used for this image, saturation was unavoidable.) Image (b) is the model image plane of the same binary optic from the design phase. First level interference spots are indicated by boxes; second level patterns by circles. The four bright cruciform patterns are the third tier patterns.

the beam combining experiment because of the noise tolerance of the phasing algorithm.<sup>2</sup>

## 2.2 Combined model

The analytical model described above, although reasonably fast for design work, suffers when it comes to control system analysis. We therefore found it useful to employ a simplified model of the binary optic (which we have called the “combined” model) when designing the control system. In effect, the analytical model was utilized to design a binary optic whose performance reasonably matched that of the combined model. The combined model was then used in image sensing and control system algorithm development.

The combined model<sup>4</sup> uses the lenslet—not the facet—as the basic unit of analysis. Recall that each facet forms a portion of a lenslet with a specific focal point. In the combined model, each lenslet is treated in isolation, as if the other lenslets were absent. Equations 1 and 2 are implemented for this simulation with the interpretation changed. Now indices  $i$  and  $j$  indicate an *adaptive optic* segment, defining wavefront—now each beam—characteristics  $I_{ij}$ ,  $\theta_{ij}$ , and  $\psi_{ij}$ . The result on the focal plane is the superposition of the electric fields that would be produced by each individual (and whole) lenslet. This is depicted in the left image of Figure 7, where an  $8 \times 8$  facet phase comparator, with four focal points, is modeled as a superposition of four separate lenses. Note that the intensity pattern produced is nearly identical with the pattern produced by the analytical model, indicating that the combined

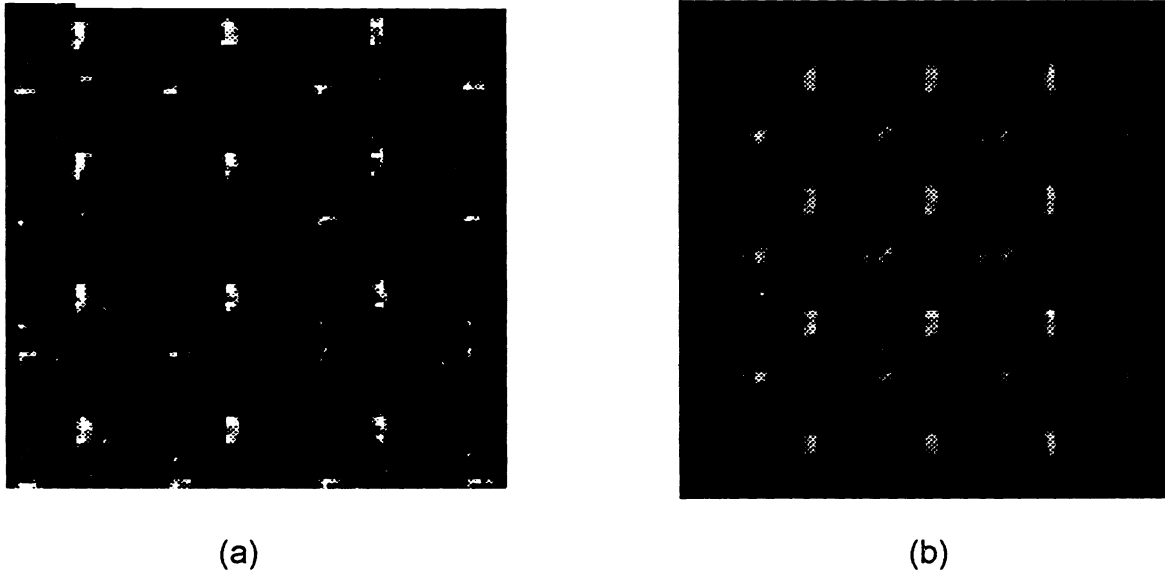


Figure 6: Actual image (a) and model image (b) for an  $128 \times 128$ ,  $8 \times 8$  beam matrix phase comparator. The images each cover a  $3 \times 3$  beam area (approximately  $1\text{mm}$  on a side). The actual image is of a somewhat planar wave, using a CCD with a slightly smaller pixel size than used in the model.

model is suitable for use in algorithm and control system development.

### 3 CONTROL MODELING

We are in the process of developing a controls system for a beam-combining testbed. In addition to the phase sensors mentioned in this paper, other sensors (such as an individual beam tip/tilt sensor) are used. Figure 8 is a block diagram of the feedback control system, which is still under development. Tip, tilt, and phase error signals are fed into the block identified as “ttp\_abc.” This block is a software calculation that breaks down the tip, tilt and phase signals into three components, namely, actuators a, b and c on the mirror. These signals are then filtered through the “Compensator” block which adjusts the magnitude and phase shift of the actuator command signals to achieve the desired closed-loop system performance.

The response of the piezoelectric actuators to the actuator commands is modeled in the “Actuator Dynamics” block—which causes the mirror to move. This movement is quantified with the “abc\_ttp” block which converts the position of each of the three actuators into a tip, tilt and phase of each mirror. As the mirror moves, the CCD camera images are modified as the light passes through the binary optics (the Hartmann sensor and phase comparator).

Finally the two CCD camera images are processed in software to measure actual tip, tilt, and phase. The measured values are then subtracted from their desired setpoints to produce the tip, tilt, and phase error signals mentioned previously.



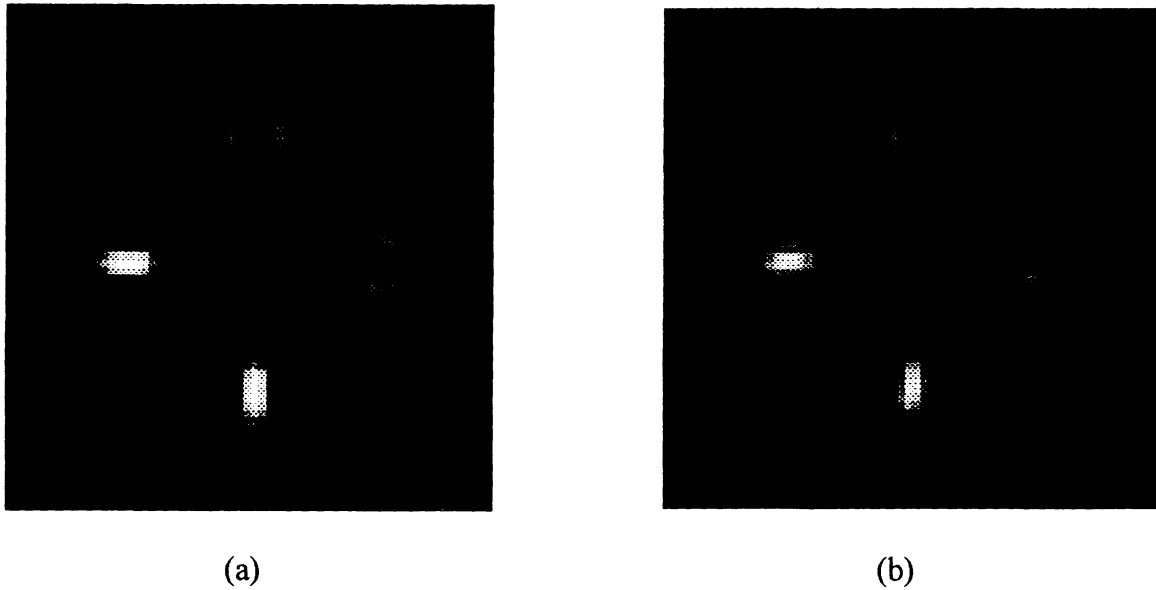


Figure 7: Comparison of combined model image (a) and analytical model image (b). A comparison indicates that the combined model—which runs much faster—is suitable for use in algorithm development for images produced by the binary optic modeled more exactly by the analytical model.

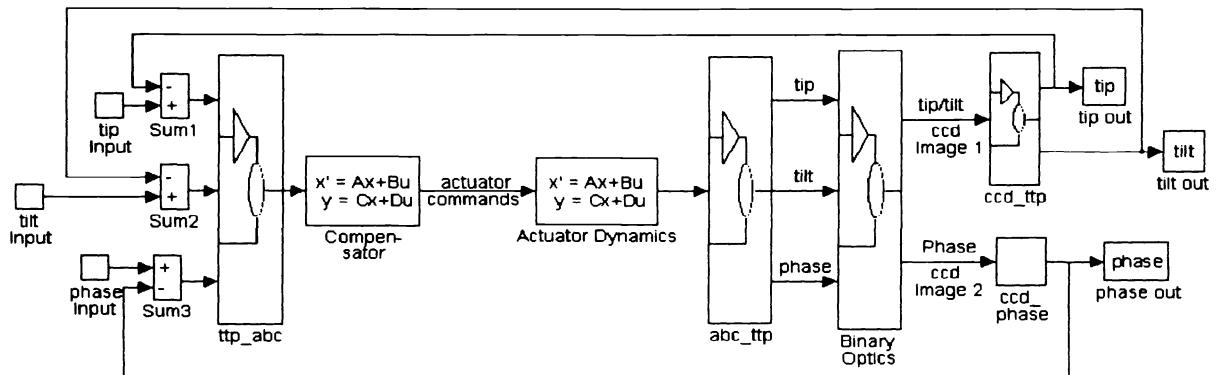


Figure 8: Block diagram of the feedback control system.

The first task in control modeling would be to *quantify* the input/output dynamics of the piezoelectric mirrors. That is, the dynamic correlation between electrical commands driving the piezo, and the actual movement of the mirror needs to be identified. This is accomplished by driving the piezo with various signals, and recording those signals, along with the output of our linear Hartmann sensor on a storage scope. From this input/output data the transfer function of the mirrors can be identified using various identification algorithms.

Because of nonlinearities in the piezo (such as hysteresis), this data needs to be collected for various scenarios. If the piezo were perfectly Linear-Time-Invariant (LTI), then each input/output data set would yield identical models. However, since all systems found in nature are somewhat nonlinear, there are always variations in the system dynamic response. The task was not only to identify the system dynamics, but also to quantify the amount of variation that can be expected from that identification due to system nonlinearities and/or time variance.

If an accurate nonlinear model of the piezo can be found, then this characterization can be exactly represented by a set of equivalent LTI transfer functions or plants, with no need for approximations nor linearizations.<sup>7</sup> If, however, no such model exists, or is inaccurate, then the characterization must be approximated by a finite set of input/output correlations. Included in the set will be input/output data that span the range of operation for the system. This technique of system characterization over a range of operation, should yield a robust control system that is optimized over that entire range. This is contrasted with the usual method of linearization about some nominal operating point which results in stable performance near that point of linearization, but can produce sub-optimum or even unstable results away from the nominal point.

Once the mirrors have been characterized, characteristics of the other components in the feedback loop will also need to be determined. These include the driving electronics, the processing time of the tip, tilt, and phase sensors, (including both the CCD cameras, and the associated software). It is expected that these characterizations will contain much less uncertainty when compared to that of the mirrors. However, (based on preliminary characterization studies) the piezo actuators are expected to have a much higher bandwidth than that of the CCD cameras and associated software. Thus, the response time of the various optical sensors is expected to be the driving factor in the design of the feedback control system. That is, the response time of the system will be limited by (and most likely equal to) the speed of the tip/tilt and phase calculations.

No measurements of the final actuators have been made yet. The actuators used in an earlier  $2 \times 2$  experiment showed a flat response to  $\sim 1$  kHz, so near-ideal performance was predicted for lower bandwidth systems. Therefore, the bulk of control modelling was done on the wavefront sensor and phase comparator models. These results are shown in the companion paper.<sup>2</sup>

## 4 ACKNOWLEDGMENTS

This work was supported by the United States Department of Energy under contract number DE-AC04-94L85000.

## 5 REFERENCES

- 1 D.R. Neal, J.D. Mansell, J.K. Gruetzner, M.E. Warren, and R. Morgan. Specialized wavefront sensors for adaptive optics. *SPIE*, 2534-32, July 1995.

- 2 D.R. Neal, S.D. Tucker, R. Morgan, T.G. Smith, M.E. Warren, J.K. Gruetzner, R.R. Rosenthal, and A.E. Bentley. Multi-segment coherent beam combining. *SPIE*, 2534-10, July 1995.
- 3 W. Goltsos and M. Holz. Agile beam steering using binary optics microlens arrays. *Opt. Eng.*, 29 11 :1392-1397, November 1990.
- 4 D. R. Neal, M. E. Warren, J. K. Gruetzner, T. G. Smith, R. R. Rosenthal, and T. S. McKechnie. A multi-tiered wavefront sensor using binary optics. *SPIE*, 2201:574-585, March 1994.
- 5 J. W. Goodman. *Introduction to Fourier Optics*. McGraw-Hill, Inc., 1968.
- 6 Inc. The MathWorks. Matlab, ver.4.0. Natick, MA, 1993.
- 7 A. E. Bentley, I. Horowitz, Y. Chait, and J. Rodrigues. Control of resistance plug welding using quantitative theory feedback. Sandia Report SAND94-0795A, Sandia National Laboratories, Albuquerque, New Mexico, 1995.